

The donor OH stretching-libration dynamics of hydrogen-bonded methanol dimers in cryogenic matrices

Matthias Heger, Jonas Andersen, Martin A. Suhm, and René Wugt Larsen

Supplementary Information

Contents

1	Ne Matrix Spectra of Deuterated Methanol Dimers	1
2	Anharmonicity Data for Deuterated Methanol Dimers	3
3	Numeric Stability Checks for VPT2 Calculations	4
3.1	Methanol Monomer	5
3.2	Methanol Dimer	6
3.3	Methanol-Ethene	7
3.4	Input for $x_{s,t} = -20 \text{ cm}^{-1}$ B3LYP calculation:	8
4	Experimental and Localized Methanol Monomer Stretching-Torsion Levels	9
5	Monomer Stretching-Torsion Couplings: Gas-Phase and Ne Matrix Data	10

1 Ne Matrix Spectra of Deuterated Methanol Dimers

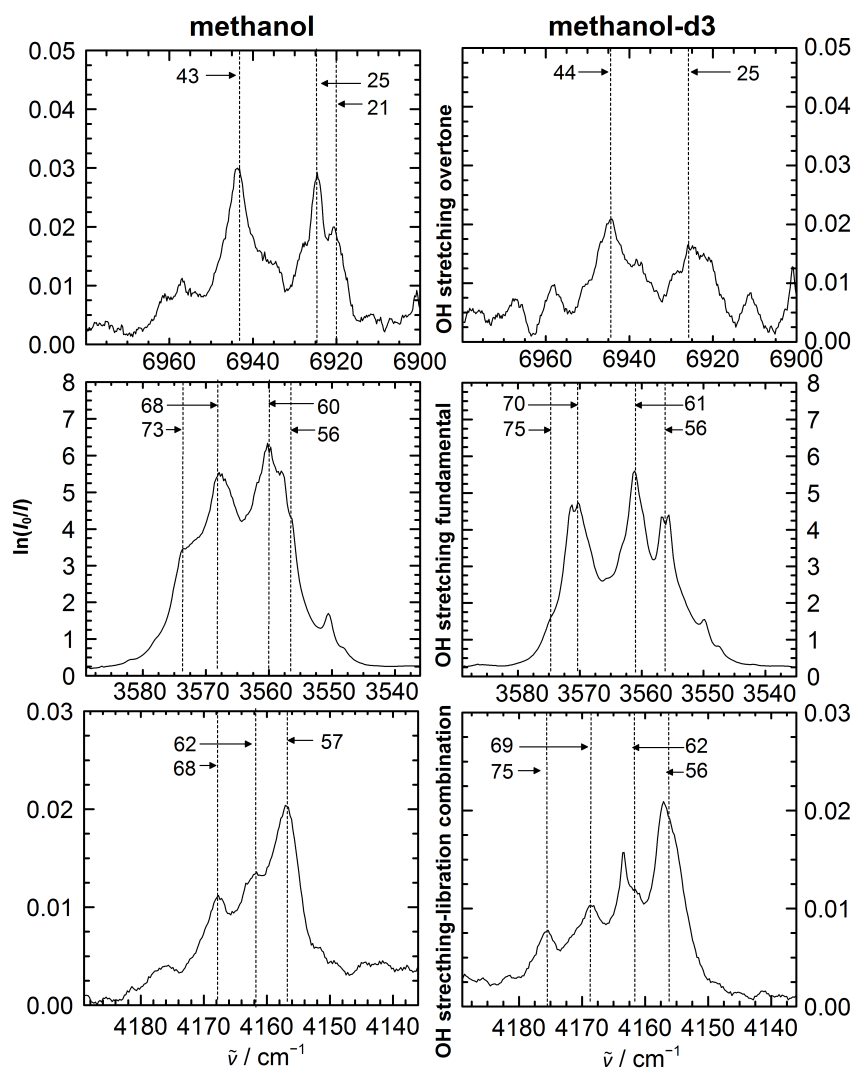


Figure S1: Ne matrix spectra of methanol and methanol-d3 in the donor OH stretching fundamental, overtone, and OH stretching-libration combination regions (from top to bottom). Annotated are the last two digits of assigned band positions.

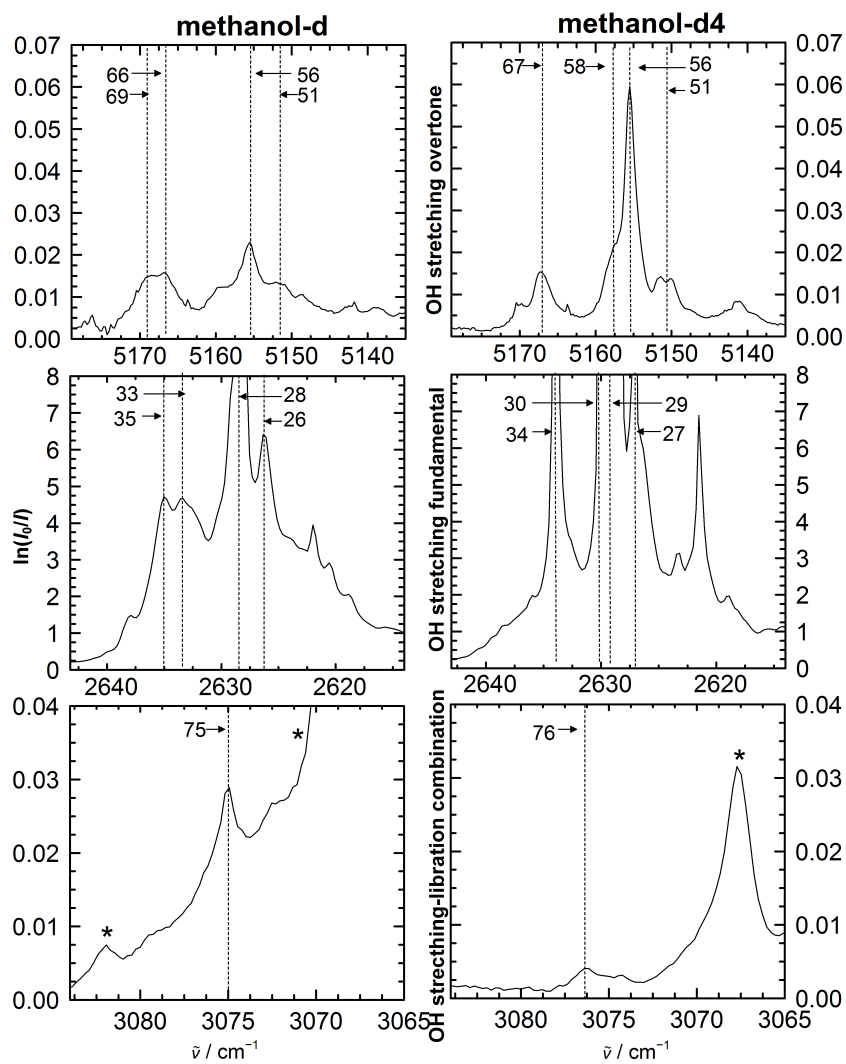


Figure S2: Ne matrix spectra of methanol-d1 and methanol-d4 in the donor OD stretching fundamental, overtone, and OD stretching-libration combination regions (from top to bottom). Annotated are the last two digits of assigned band positions. Asterisks mark monomer bands.

2 Anharmonicity Data for Deuterated Methanol Dimers

Table S1: Predicted and observed anharmonicity constants for the methanol-d1, -d3 and -d4 dimers for diagonal OH/OD donor stretching ($x_{s,s}$) and libration ($x_{l,l}$) anharmonicity, and stretching-libration couplings ($x_{s,l}$). See Ref. [1] for the methanol-d1 fundamental band position. The Ne matrix data are obtained from correlating the sub-bands displayed in Figs. S1 and S2. For methanol-d1 and -d4, we refrain from deducing coupling constants due to ambiguous combination band assignments (see the main text). All data in cm^{-1} .

	$x_{s,s}$	$x_{l,l}$	$x_{s,l}$
methanol-d1			
B2PLYP-D3/VTZ	-54	-21	+30
B3LYP-D3/VTZ	-55	-22	+30
MP2/VTZ	-53	-23	+30
exp. (Ne)	-51	-37	
	-50		
	-50		
	-51		
methanol-d3			
B2PLYP-D3/VTZ	-102	-41	+57
B3LYP-D3/VTZ	-104	-43	+57
MP2/VTZ	-102	-45	+60
exp. (Ne)	-98		+42
	-99		+41
			+43
			+42
methanol-d4			
B2PLYP-D3/VTZ	-54	-23	+29
B3LYP-D3/VTZ	-55	-24	+29
MP2/VTZ	-53	-24	+30
exp. (Ne)	-51		
	-51		
	-51		
	-52		

3 Numeric Stability Checks for VPT2 Calculations

Previously, VPT2 studies on the anharmonic vibrational dynamics in the methanol dimer [2, 1] and methanol-ethene [3] have been presented using DFT methods in conjunction with Grimme’s D3 dispersion correction [4] and Becke-Johnson damping [5]. Due to potential incompatibilities of the latter with the VPT2 code, we have carried out all calculations in the current project with only zero-damping. However, we still find the DFT results to be unstable with respect to chosen molecular structures and optimizations (calculations II to IV in Tabs. S2 to S4 below), while MP2 behaves better in this regard. Further, inconsistencies arise for methanol monomers and dimers when the anharmonic calculations are done either directly succeeding the geometry optimization in a single run, or when using the nominally equivalent pre-optimized structures from checkpoint files (compare calculations I and IV in the tables below). While the first issue hints towards problems with numerical DFT integration grids, the second one persists also for MP2 and possibly suggests rounding effects upon storage and recovery of data from the program’s checkpoint files. The latter inconsistencies are, however, systematically reproducible when repeating the calculations.

Curiously, one B3LYP calculation – the input of which is reproduced below the following tables – suggests a stretching-torsion coupling of -20 cm^{-1} , which even upholds for slight variations of the geometry. This result is clearly an outlier and appears to be caused by the Coriolis contributions. Still, it provides a striking example of the high sensitivity of the DFT/VPT2 combination to unfortunate choices of starting structures. What is more, the mixed methanol-ethene dimer that we have investigated previously [3] (see Tab. S4) shows much larger deviations concerning the low-lying modes than the methanol homodimer, which is plausible seeing that already the harmonic treatment often fails to correctly predict the lowest intermolecular mode, corresponding to a torsion of the ethene molecule around the hydrogen bond. However, the stretching-libration coupling constant $x_{s,l}$ is again robust.

Seeing the earlier methanol dimer results in Refs. [1] and [2], we thus propose error bars of $\pm 5\text{ cm}^{-1}$ for OH stretching and $\pm 10\text{ cm}^{-1}$ for OH libration wavenumbers, and up to $\pm 20\text{ cm}^{-1}$ for off-diagonal sums, with the latter mostly ascribable to couplings to intermolecular modes (cf. the last row of Tab. S3). The overall findings are, however, still within reasonable bounds, irrespective of the use of Becke-Johnson damping. For methanol-ethene [3], we have not concentrated on the librational band itself so far; while the variations for the OH stretching band and the primed anharmonic sum appear to be somewhat larger than in the methanol case, our earlier comparison between theory and experiment still appears realistic. As a side note, the spurious checkpoint file inconsistencies are absent for MP2 in this case.

3.1 Methanol Monomer

Table S2: Numeric stability tests for anharmonic VPT2 calculations of the methanol monomer, demonstrated on band positions and anharmonicity constants for the donor OH stretching and torsion bands (see the main text for details). Harmonic wavenumbers are further supplied for both vibrations. All DFT data were obtained using an ultrafine integration grid (“int=ultrafine”) and zero-damping.

	MP2			B2PLYP-D3				B3LYP-D3			
	I	II	IV	I	II	III	IV	I	II	III	IV
ω_s	3882	3882	3882	3858	3858	3858	3858	3829	3829	3829	3829
$\tilde{\nu}_s$	3706	3706	3706	3674	3674	3675	3674	3645	3645	3647	3645
ω_t	309	309	309	307	307	307	307	306	306	306	306
$\tilde{\nu}_t$	257	256	256	241	243	243	242	233	236	234	232
$\sum x_{s,i}$	-21	-21	-21	-24	-24	-22	-24	-22	-22	-17	-22
$\sum' x_{s,j}$	-30	-30	-30	-28	-28	-28	-28	-26	-25	-26	-26
$x_{s,s}$	-83	-83	-83	-86	-86	-86	-86	-87	-87	-87	-87
$x_{s,t}$	+9	+9	+9	+4	+4	+5	+4	+3	+4	+8	+3
$x_{t,t}$	-30	-31	-31	-35	-34	-34	-35	-37	-36	-37	-37
$\sum' x_{t,j}$	+9	+8	+9	+3	+5	+5	+4	-2	0	-3	-2

I: Optimized using “opt=tight”.

II: Using stored structures (“geom=checkpoint”) from calculations I, re-optimized using “opt=verytight”.

III: Optimized using “opt=verytight”, starting from alternative structures.

IV: Using stored structures (“geom=checkpoint”) from calculations I without re-optimization.

3.2 Methanol Dimer

Table S3: Numeric stability tests for anharmonic VPT2 calculations of the methanol dimer, demonstrated on band positions and anharmonicity constants for the donor OH stretching and libration bands (see the main text for details). “ $\tilde{\nu}_2$ ” and “ $2\tilde{\nu}_2$ ” denote the fundamental and first overtone of the (harmonically) second-lowest vibration, found to be most sensitive to displacements. Harmonic wavenumbers ω are further supplied for the given vibrations. All DFT data were obtained using an ultrafine integration grid (“int=ultrafine”) and zero-damping. The last line gives the summed coupling terms of the libration to the seven lowest-frequency modes.

	MP2			B2PLYP-D3				B3LYP-D3			
	I	II	IV	I	II	III	IV	I	II	III	IV
ω_s	3740	3740	3740	3722	3722	3722	3722	3687	3687	3687	3687
$\tilde{\nu}_s$	3571	3571	3571	3554	3557	3559	3557	3520	3523	3507	3514
ω_1	699	699	699	697	697	697	697	700	700	700	700
$\tilde{\nu}_1$	592	592	594	589	594	613	600	586	596	556	575
ω_2	56	56	56	60	60	60	60	53	53	53	53
$\tilde{\nu}_2$	36	36	16	11	108	6	23	2	10i	12i	10i
$2\tilde{\nu}_2$	43	43	2i	8i	207	20i	17	30i	60i	55i	53i
$\tilde{\nu}_{s,1}$	4222	4222	4225	4200	4209	4230	4215	4164	4178	4120	4147
$\sum x_{s,i}$	+68	+68	+68	+73	+79	+83	+79	+83	+90	+58	+72
$\sum' x_{s,j}$	+9	+9	+9	+15	+22	+26	+22	+25	+32	+0	+14
$x_{s,s}$	-102	-102	-102	-102	-102	-102	-102	-104	-104	-104	-104
$x_{s,1}$	+59	+59	+59	+58	+58	+58	+58	+58	+58	+58	+58
$x_{1,1}$	-46	-46	-46	-43	-43	-43	-43	-45	-45	-46	-46
$\sum x_{1,1\dots7}$	-71	-71	-66	-80	-71	-40	-61	-85	-68	-134	-103

I: Optimized using “opt=tight”.

II: Using stored structures (“geom=checkpoint”) from calculations I, re-optimized using “opt=verytight”.

III: Optimized using “opt=verytight”, starting from alternative structures.

IV: Using stored structures (“geom=checkpoint”) from calculations I without re-optimization.

3.3 Methanol-Ethene

Table S4: Numeric stability tests for anharmonic VPT2 calculations of the mixed methanol-ethene dimer, demonstrated on band positions and anharmonicity constants for the donor OH stretching and libration bands. “ $\tilde{\nu}_1$ ” denotes the fundamental transition of the lowest vibration, corresponding to a torsion of the ethene molecule around the hydrogen bond. Harmonic wavenumbers ω are further supplied for the given vibrations. All DFT data were obtained using an ultrafine integration grid (“int=ultrafine”) and zero-damping.

	MP2		B2PLYP-D3		B3LYP-D3	
	I	IV	I	III	I	III
ω_s	3823	3823	3805	3805	3776	3776
$\tilde{\nu}_s$	3652	3652	3633	3622	3601	3604
ω_l	448	448	431	431	425	425
$\tilde{\nu}_l$	372	372	383	295	324	346
ω_1	15	15	19	19	12	12
$\tilde{\nu}_1$	22	22	14	45i	206i	16i
$\sum x_{s,i}$	+12	+12	+20	-2	+19	+23
$\sum' x_{s,j}$	-4	-4	+6	-15	+1	+5
$x_{s,s}$	-88	-88	-91	-91	-92	-92
$x_{s,l}$	+17	+17	+14	+13	+18	+18

I: Optimized using “opt=tight”.

III: Optimized using “opt=verytight”, starting from alternative structures.

IV: Using stored structures (“geom=checkpoint”) from calculations I without re-optimization.

3.4 Input for $x_{s,t} = -20 \text{ cm}^{-1}$ B3LYP calculation:

```
#t b3lyp empiricaldispersion=gd3 cc-pvtz int=ultrafine opt=tight freq=anharm
```

```
Methanol monomer, opt+freq anharm
```

```
0 1
```

```
C -2.25493200 0.13438100 0.32597700
```

```
O -1.27042600 -0.43651400 -0.51149500
```

```
H -2.45283100 1.17908700 0.07494300
```

```
H -1.98003000 0.07716000 1.38187900
```

```
H -3.17164500 -0.43100900 0.18051100
```

```
H -0.44245400 0.04482500 -0.37662100
```

4 Experimental and Localized Methanol Monomer Stretching-Torsion Levels

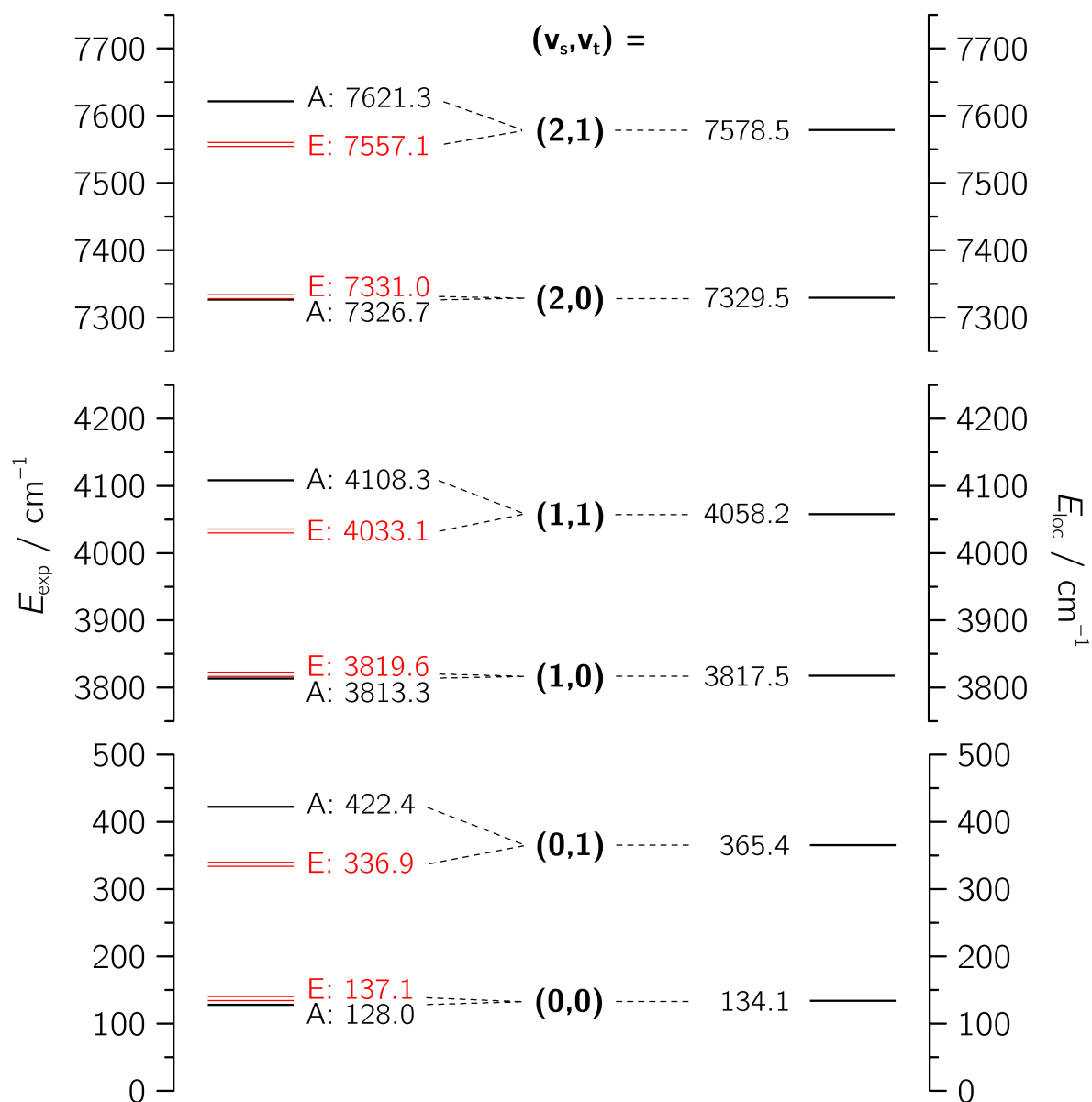


Figure S3: Stretching-torsion levels in the methanol monomer as taken from Refs. [6, 7, 8] (E_{exp} , left) and localized to a single potential minimum using a simple state-specific scheme (E_{loc} , right).

5 Monomer Stretching-Torsion Couplings: Gas-Phase and Ne Matrix Data

In his Ne matrix studies [9, 10], Perchard gives a 3915.5 cm^{-1} for the stretching-torsion combination band in Table 7 of Ref. [10], but without making the involved torsional sub-levels explicit. In the same paper, Table 1 lists the fundamental transitions for the torsion and stretching modes as 212.5 and 3690.2 cm^{-1} , respectively. Drawing from Table 2 in Ref. [9], it is clear that these wavenumbers belong to the E←A torsion and A←A stretching transitions; this indicates that the combination band also stems from an E←A transition. The stretching-torsion coupling derived from these wavenumbers is $+12.8\text{ cm}^{-1}$. (Note that for some reason, Ref. [10] states a $+13.1\text{ cm}^{-1}$ result using the same band positions.)

Further, Table 2 in Ref. [9] indicates that the deviations between Ne matrix and gas-phase wavenumbers for the stretching and torsion bands are moderate (on the order of $\pm 5\text{ cm}^{-1}$). From the gas-phase monomer data by Hunt *et al.* [6], we infer a stretching-torsion combination wavenumber of 3905.1 cm^{-1} for the transition from the $v_s, v_t = 0, 0$ A to the $1, 1$ E level. Together with the gas-phase fundamental transitions of 208.9 cm^{-1} and 3685.3 cm^{-1} , this yields a stretching-torsion coupling of $+10.9\text{ cm}^{-1}$. Among all possible sub-level combinations, this E←A transition is in closest agreement to the Ne matrix combination band suggested by Perchard, consistent with his own choice of sub-bands in Ref. [10].

References

- [1] F. Kollipost, J. Andersen, D. W. Mahler, J. Heimdal, M. Heger, M. A. Suhm, and R. Wugt Larsen. The effect of hydrogen bonding on torsional dynamics: a combined far-infrared jet and matrix isolation study of methanol dimer. *J. Chem. Phys.*, 141:174314, 2014.
- [2] Franz Kollipost, Kim Papendorf, Yu-Fang Lee, Yuan-Pern Lee, and Martin A. Suhm. Alcohol dimers – how much diagonal OH anharmonicity? *Phys. Chem. Chem. Phys.*, 16:15948–15956, 2014.
- [3] Matthias Heger, Ricardo A. Mata, and Martin A. Suhm. Soft hydrogen bonds to alkenes: The methanol–ethene prototype under experimental and theoretical scrutiny. *Chem. Sci.*, 6:3738–3745, 2015.
- [4] Stefan Grimme, Jens Antony, Stephan Ehrlich, and Helge Krieg. A consistent and accurate ab initio parametrization of density functional dispersion correction (DFT-D) for the 94 elements H-Pu. *J. Chem. Phys.*, 132:154104, 2010.
- [5] Stefan Grimme, Stephan Ehrlich, and Lars Goerigk. Effect of the damping function in dispersion corrected density functional theory. *J. Comput. Chem.*, 32:1456–1465, 2011.
- [6] R. H. Hunt, W. N. Shelton, Francis A. Flaherty, and W. B. Cook. Torsion–Rotation Energy Levels and the Hindering Potential Barrier for the Excited Vibrational State of the OH–Stretch Fundamental Band ν_1 of Methanol. *J. Mol. Spectrosc.*, 192:277–293, 1998.
- [7] D. Rueda, O. V. Boyarkin, T. R. Rizzo, I. Mukhopadhyay, and D. S. Perry. Torsion–rotation analysis of OH stretch overtone–torsion combination bands in methanol. *J. Chem. Phys.*, 116:91–100, 2002.
- [8] Giovanni Moruzzi, Franco Strumia, Jaão Carlos Silos Moraes, Ronald M. Lees, Indranath Mukhopadhyay, John W.C. Johns, Brenda P. Winnewisser, and Manfred Winnewisser. The spectrum of CH₃OH between 200 and 350 cm⁻¹: Torsional transitions and evidence for state mixings. *J. Mol. Spectrosc.*, 153:511–577, 1992.
- [9] J. P. Perchard. The torsion-vibration spectrum of methanol trapped in neon matrix. *Chem. Phys.*, 332:86–94, 2007.
- [10] J. P. Perchard, F. Romain, and Y. Bouteiller. Determination of vibrational parameters of methanol from matrix-isolation infrared spectroscopy and ab initio calculations. Part 1 – Spectral analysis in the domain 11000–200cm⁻¹. *Chem. Phys.*, 343:35–46, 2008.